THEORETICAL AND EXPERIMENTAL COMPARISON BETWEEN TUNED LOAD AND CLASS-F POWER AMPLIFIERS

LADY FERNANDA PEREZ MANCERA
NORMA RESTREPO BURGOS

Thesis submitted for the fulfillment of the requirements for the degree of

ELECTRONIC ENGINEER

Director:
JORGE JULIAN MORENO RUBIO
Thesis Director

UNIVERSIDAD PEDAGOGICA Y TECNOLOGICA DE COLOMBIA
FACULTAD SECCIONAL SOGAMOSO
ESCUELA DE INGENIERIA ELECTRONICA
SOGAMOSO
2014

APPROVAL GRADE

_____

_____

_____

_____

_____

JORGE JULIAN MORENO RUBIO PH.D.
Thesis Director

_____

COMMITTEE MEMBER

_____

COMMITTEE MEMBER

UNIVERSIDAD PEDAGOGICA Y TECNOLOGICA DE COLOMBIA
FACULTAD SECCIONAL SOGAMOSO
ESCUELA DE INGENIERIA ELECTRONICA
SOGAMOSO, August 2014

ACKNOWLEDGMENTS

The realization of this project was possible due to many people's collaboration, whom we desire to express our gratefulness.

We acknowledge especially the support, patience and guidance of our friends Julián Rodriguez and William Cuevas, members of research group GINTEL.

We wish to express our most sincere gratitude and appreciation to PhD Jorge Julián Moreno Rubio, who has been the ideal thesis director.

We would like to thank from a special way to our friend, Henry Panteviz for letting us to use his laser printer.

To PhD Liliana Fernández, we are grateful for the advising, motivation and the trust deposited in us to face this challenge.

Thanks also go to the engineers Oscar Hernandez for lending us his soldering station and Oscar Higuera for helping us to make the book format.

Lastly, we would like to express our sincere appreciation to all people involved in the amplifiers implementation, for their outstanding efforts.

DEDICATION

This thesis is dedicated to our loving parents and siblings who have supported us throughout the process, and have given us words of encouragement and push, and also to God the Divine who made it possible.

INTRODUCTION

Modern communication systems in last decade have faced some challenges as the development of new communication standards and protocols demanding to grant greater services with the limited frequency resources, therefore new types of communication have been develop such as WiFi operating at 2.4GHz, it is a frequency used in some countries by fourth generation systems 4G and probably it will be used by fifth generation systems [1, 2].

A high efficiency power amplifier (PA) is fundamental in the wireless communication system transmitter for minimizing DC power dissipating, on the contrary, it gives rice the cooling requirements and devices and batteries size increase [3, 4].

PA design techniques include some based on harmonic manipulation such as Tuned Load (TL) and Class F. The TL design consists in terminating the device output with short-circuit terminations at harmonic frequencies, as a result, a sinusoid output voltage waveform is generated from the imposed half-sinusoid output current waveform. In class F mode, the load has to be open at odd harmonics and short at even harmonics. Ideally it is characterized for having 100% of efficiency due to no overlapping between the drain current and voltage waveforms, obtaining no power dissipation [5, 6].

This document presents the principles of these two high efficiency power amplifiers. Then the design methodology and realization based on the same active device are described. Finally, the obtained results that show the performance especially of drain efficiency, gain and output power are compared between both amplifiers.

PROBLEM IDENTIFICATION

The modern communication systems have been developed, to support the increase users amount and to grant greater services in data transmission with the limited frequency resources [1]. A PA is an essential component in this kind of systems, which is the responsible of most energy consumption, and in this way is directly related to the cost of the transmission [5, 7].

Some figures of merit characterizing a PA are efficiency, gain and output power. The researchers effort is centered in finding a trade-off between these characteristics to obtain reliability in the transmission and smaller and lower cost circuit [1, 5, 8].

Many design methods and architectures for PA have been proposed, with the purpose of surpassing the problem of energy wasting [9]. The Tuned load is a model based on the design of harmonic loads in power amplifiers, which can be modified to obtain a PA of higher efficiency such as the class F which is one of the most mentioned in literature [6].

With this proposal some concepts of PA design are demonstrated through a theoretical and practical comparison between a Tuned load and a class F PAs, to create a resource of researching in microwave and radio frequency at the *Universidad Pedagógica y Tecnológica de Colombia (UPTC)* in *Sogamoso* and in this way to determine which are the advantages and disadvantages of a Tuned load PA with respect to a class F PAs.

JUSTIFICATION

The telecommunications research group GINTEL wants to encourage research in electronic engineering academic community, especially in the radio frequency and microwaves, in this case studying high efficiency PAs.

The most important PA figures of merit are efficiency, gain and output power. High efficiency decreases heat dissipation causing the presence of promoting effects such as prolongation of life devices, decrease transmission cost, avoiding the inclusion of cooling systems and prototype size reduction [5].

Single-stage amplifiers can be used to build more complex amplifiers with multiple stages such as Doherty PA (DPA). When counting in the group GINTEL with single stage PAs to commercial frequencies, for example to Wi-Fi and WiMAX applications, it will facilitate further works in this topic.

OBJECTIVES

GENERAL OBJECTIVE

To develop strategies for designing, manufacturing and characterization of single stage high efficient power amplifiers, using GaN devices (Gallium Nitrate), for applications in wireless communication systems.

SPECIFIC OBJECTIVES

- To design a Tuned load and a class F PAs at 2.4 GHz.
- To simulate Tuned load and class F PAs using Advanced Design System of Agilent.
- To implement Tuned load and class F PAs using Cree's CGH40010 devices.
- To make theoretical and experimental comparison of efficiency, gain and power between Tuned load and class F PAs.

Contents

List of Figures

List of Tables

Chapter 1

POWER AMPLIFIER FUNDAMENTALS

1.1 Definition

The PA is one of the three main categories of amplifiers used in wireless systems. It is located in the output stage of a transmitter and used to increase the radiated power level [10]. The Fig. 1.1 shows the simple analog architecture scheme of the wireless communication system transmitter, where data modulates a high-frequency carrier, this result is subsequently amplified through a PA and radiated by the antenna [11].

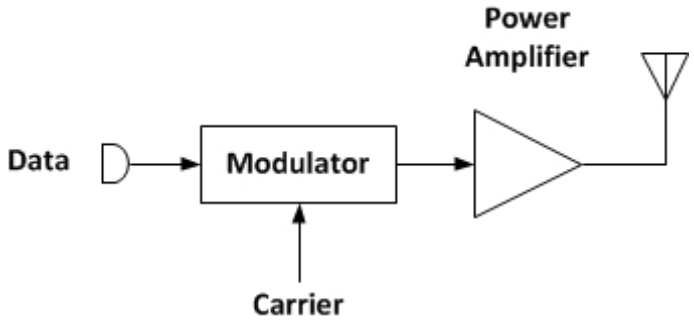

Figure 1.1: Block diagram of a generic analog transmitter.

The main figures of merit characterizing the PA behavior such as gain, power and efficiency are defined in the following sections together with other important design parameters like stability.

1.2 Scattering Parameters

A PA can be represented by a two port network, the behavior of which can be characterized by scattering parameters (S parameters) allowing easier analysis. The S parameters can be measured accurately at high frequency and are defined in terms of traveling waves [12].

The voltage and current in a lossless transmission line are given by the equations:

$$V(x) = Ae^{-j\beta x} + Be^{j\beta x} \tag{1.1}$$

and

$$I(x) = \frac{A}{Z_o}e^{-j\beta x} - \frac{B}{Z_o}e^{j\beta x} \tag{1.2}$$

The normalized incident voltage wave $a(x)$ and the normalized reflected voltage wave $b(x)$ are:

$$a(x) = \frac{1}{2\sqrt{Z_o}}[V(x) - Z_o I(x)] \tag{1.3}$$

and

$$b(x) = \frac{1}{2\sqrt{Z_o}}[V(x) + Z_o I(x)] \tag{1.4}$$

The two-port network shown in Fig. 1.2 has an incident wave $a_1(x)$ and a reflected wave $b_1(x)$ at port 1, which is located at $x_1 = l_1$, and an incident wave $a_2(x)$ and a reflected wave $b_2(x)$ at port 2, which is located at $x_2 = l_2$.

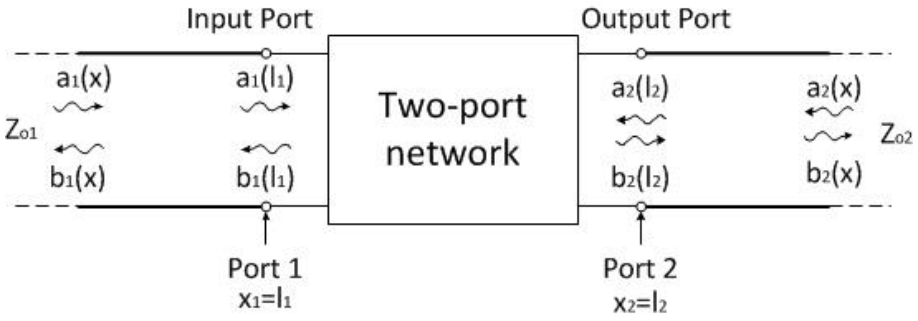

Figure 1.2: Incident and reflected waves in a two-port network.

Reflected waves can be written in terms of incident waves, it can be express in matrix form as shown in 1.5.

$$\begin{bmatrix} b_1(l_1) \\ b_2(l_2) \end{bmatrix} = \begin{bmatrix} S_{11} & S_{12} \\ S_{21} & S_{22} \end{bmatrix} \begin{bmatrix} a_1(l_1) \\ a_2(l_2) \end{bmatrix} \tag{1.5}$$

being S_{11}, S_{12}, S_{21} and S_{22} the S parameters measured at ports 1 and 2, which represent reflection and transmission coefficients and form the scattering matrix which gives a linear model of the two-port network, where

S_{11} is the input reflection coefficient with output properly terminated.

$$S_{11} = \frac{b_1(l_1)}{a_1(l_1)} \mid_{a_2(l_2)=0} \tag{1.6}$$

S_{12} is the reverse transmission coefficient with input properly terminated.

$$S_{12} = \frac{b_1(l_1)}{a_2(l_2)} \mid_{a_1(l_1)=0} \tag{1.7}$$

S_{21} is the forward transmission coefficient with output properly terminated.

$$S_{21} = \frac{b_2(l_2)}{a_1(l_1)} \mid_{a_2(l_2)=0} \tag{1.8}$$

S_{22} is the output reflection coefficient with input properly terminated.

$$S_{22} = \frac{b_2(l_2)}{a_1(l_1)} \mid_{a_1(l_1)=0} \tag{1.9}$$

1.3 Power

The output power is one the parameters that describe the PA's performance, it is characterized for being higher than the input power and used to define other important parameters such as the gain and efficiency [5]. The Fig. 1.3 shows a microwave amplifier with traveling waves a_1, b_1 , a_2 and b_2. The source reflection coefficient in a Z_o system is given by:

$$\Gamma_S = \frac{Z_S - Z_o}{Z_S + Z_o} \tag{1.10}$$

and the input reflection coefficient is:

$$\Gamma_{IN} = \frac{b_1}{a_1} \tag{1.11}$$

The power delivered to the input port of the transistor is [5, 10]

$$P_{IN} = \frac{1}{2} Re(V_{IN} I_{IN}^*) \tag{1.12}$$

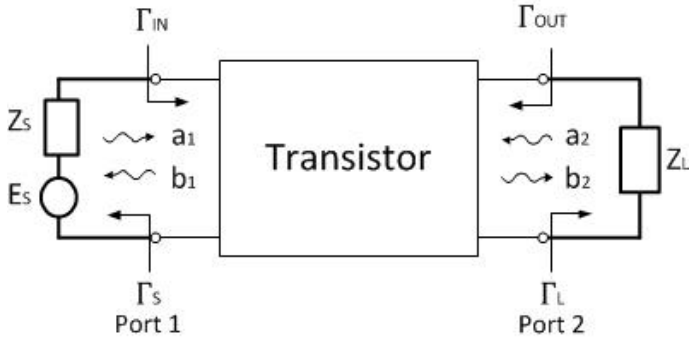

Figure 1.3: Block diagram of a microwave amplifier.

The power available from the source is the maximum power that can be delivered to the network. It is equal to the input power when $\Gamma = (\Gamma)^*$ and is given by:

$$P_{AVS} = \frac{\frac{1}{2}|b_S|^2}{1 - |\Gamma_S|^2} \tag{1.13}$$

where

$$b_S = \frac{E_S\sqrt{Z_o}}{Z_S + Z_o} \tag{1.14}$$

The output power P_{OUT} is the power delivered to the load Z_L given by:

$$P_{OUT} = \frac{1}{2}Re(V_{OUT}I^*_{OUT}) \tag{1.15}$$

An alternative definition is the power added P_{ADD}, which takes into account of the contribution of the output power coming directly from the input [5, 13]

$$P_{ADD} = P_{OUT} - P_{IN} \tag{1.16}$$

Usually power quantities are expressed in logarithmic units called $dBms$:

$$P_{dBm} = 10log_{10}(P_W) + 30 \tag{1.17}$$

where P_W is power given by Watts.

1.4 Gain

Three different types of power gains are defined in two-port network theory (Fig. 1.3) [10] :

The operating power gain is defined as the ratio between output and input power:

$$G_P = P_{OUT}/P_{IN} \tag{1.18}$$

The transducer power gain is the ratio between output power and power available from the source. It depends on both Z_S and Z_L:

$$G_T = P_{OUT}/P_{AVS} \tag{1.19}$$

The available power gain is the ratio between power available from the source and power available from the network. It depends on Z_S but not Z_L:

$$G_A = P_{AVN}/P_{ANS} \tag{1.20}$$

In a similar way of power, a logarithmic unit is used (called dB):

$$G_{dB} = 10log_{10}(G) = P_{OUT}[dBm] - P_{IN}[dBm] \tag{1.21}$$

1.5 Efficiency

The effectiveness with which the amplifier converts DC power from supplies into microwave power is known as efficiency. It is one of the important parameters in specifying general system performance [5,14]. Low efficiency leads to high power consumption, increase cooling requirements, big battery and prototype size and high cost of the transmission [3]. The efficiency η is usually expressed as a percentage and it is defined as the ratio of RF output power to supplied DC power:

$$\eta\% = \frac{P_{OUT}}{P_{DC}} * 100 \tag{1.22}$$

Since most power amplifiers have relatively low gains because of the high frequency, the power added efficiency (PAE) takes the effect of RF power delivered at the input into account, which defined as the ratio between the added power and the supplied DC power [5, 10]:

$$\eta_{add}\% = \frac{P_{ADD}}{P_{DC}} * 100 \tag{1.23}$$

1.6 Stability

In a PA, its stability or resistance to oscillate is one of the key issues in the design, since oscillations affect the normally working and performance of the amplifier [15]. It depends on the frequency and can be determined from S parameters, the matching networks and the terminations. As the amplifier can be stable at the design frequency, but unstably at different frequencies, the overall amplifier stability has to be enforced for all frequencies. Stability problems are also very dependent on the device type [5, 10–12, 16]. In the two-port network in Fig. 1.3, oscillations can be presented having a negative resistance in the input or output port. It involves $|\Gamma_{IN}| > 1$ or $|\Gamma_{OUT}| > 1$, because Γ_{IN} and Γ_{OUT} depend on the source and load matching networks.

Two types of stability can be defined. The network is unconditionally stable if $|\Gamma_{IN}| < 1$ and $|\Gamma_{OUT}| < 1$ for all passive source and load impedances. The network is conditionally stable or potentially unstable if $|\Gamma_{IN}| < 1$ and $|\Gamma_{OUT}| < 1$ only for a certain range of passive source and load impedances. The amplifier is unconditionally stable when the *Rollet's condition* is satisfied [10]:

$$K \hat{=} \frac{1 - |S_{11}|^2 - |S_{22}|^2 + |\triangle|^2}{2|S_{12}S_{21}|^2} > 1 \tag{1.24}$$

and

$$|\triangle| < 1 \tag{1.25}$$

where

$$\triangle \hat{=} S_{11}S_{22} - S_{12}S_{21} \tag{1.26}$$

1.7 Power Devices

High power devices require a suitable internal thermal balance which depends on properties of semiconductor materials and their distribution into the device. A variety of RF solid state devices with different features have been developed, being the High Electron Mobility Transistors (HEMTs) one of the improved structures. GaN is a wide bandgap material, their properties compared to main substrates are reported in Table 1.1.

The energy bandgap is the minimum energy needed to excite and transfer an electron from the valence to conduction bands in the semiconductor, therefore this material has high

Material	Mobility $[\frac{cm^2}{V.s}]$	Dielectric Constant $[\varepsilon]$	Bandgap [eV]	Breakdown field $[Eb10^6 V/cm]$	T_{max} [C]
Si	1300	11.9	1.12	0.3	300
GaAs	5000	12.5	1.42	0.4	300
4H-SiC	260	10.0	3.20	3.5	600
GaN	1500	9.5	3.40	2.0	700

Table 1.1: Material properties of microwave semiconductors.

operation temperature, efficiency, power density, immunity to external influences, operating voltage and supports high internal electric fields before the electronic breakdown event with small device size [5, 17].

Chapter 2

TUNED LOAD AMPLIFIER

The TLPA is a strategy which offers more efficiency in comparison of quasi-linear conventional approaches like class A and class B. It is usually used as reference to compare and evaluate more efficient schemes [5, 18].

The TL technique working consist of setting short-circuit terminations at the harmonic frequencies in the active device, maximizing fundamental-frequency voltage and current swings [5]. The tuned load loading scheme is depicted in Fig. 2.1

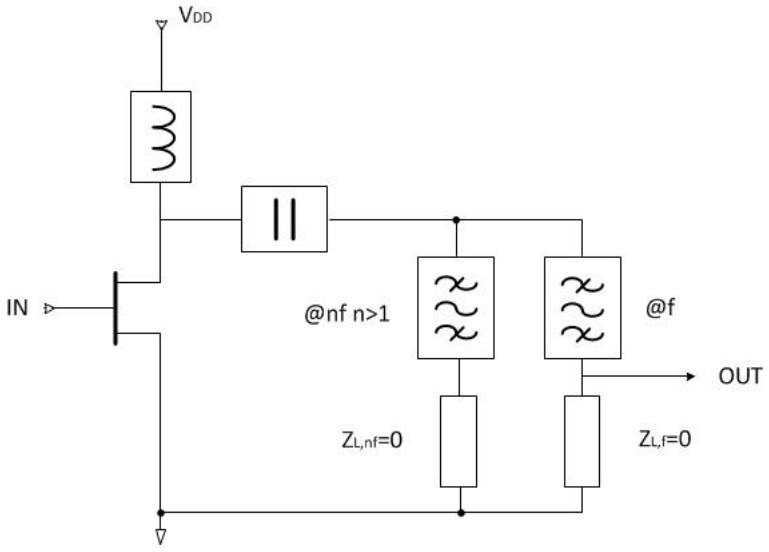

Figure 2.1: The tuned load loading scheme.

When its maximum swing is reached, the resulting output current waveform $I_D(t)$ is a truncated sinusoidal given by:

$$I_D(t) = \begin{cases} \dfrac{I_{max}}{1 - cos(\frac{\theta}{2})} * [cos(\omega t) - cos(\frac{\theta}{2}) & \text{if } |\omega t| \leq 0 \\ 0 & \text{otherwise} \end{cases} \tag{2.1}$$

where $\omega = 2\pi f$ and θ is the drain Current Conduction Angle (CCA). The CCA is connected with the ratio between the quiescent DC bias current I_Q and the maximum current I_{max}:

$$\cos\frac{\theta}{2} = \frac{\xi}{\xi - 1} \tag{2.2}$$

where

$$\xi = \frac{I_Q}{I_{max}} \tag{2.3}$$

With the short-circuit terminations at all harmonic frequencies, the output drain voltage waveform $V_{DS}(t)$ is purely sinusoidal. It can be expressed as:

$$V_{DS}(t) = V_{ds,DC} - V_1 \cos(\omega t) \tag{2.4}$$

where $V_{ds,DC}$ is the drain voltage and V_1 is the fundamental harmonic component, it is:

$$V_1 = \frac{V_{ds,DC} - V_k}{2} \frac{\pi}{\pi - 1} \tag{2.5}$$

The optimum load at fundamental frequency $R_{TL}(\theta)$ is given by [19]

$$R_{TL}(\theta) = \frac{V_{ds,DC} - V_k}{I_1(\theta)} \tag{2.6}$$

where V_k is the device knee voltage and $I_1(\theta)$ is the fundamental component of the truncated sinusoidal drain current at its maximum swing with a conduction angle of θ, this current can be calculated as

$$I_1(\theta) = \frac{I_{max}}{2\pi} \frac{\theta - \sin\theta}{1 - \cos\frac{\theta}{2}} \tag{2.7}$$

The DC power $P_{DC,TL}$, the output power at the fundamental frequency $P_{OUT,TL}$ and the drain efficiency η_{TL} are given by the following expressions [5]:

$$P_{DC,TL} = I_o V_{ds,DC} = \frac{P_{DC,A}}{\pi} \frac{2\sin\frac{\theta}{2} - \theta\cos\frac{\theta}{2}}{1 - \cos\frac{\theta}{2}} \tag{2.8}$$

where $I_0(\theta)$ is the DC component of the truncated drain current, it is:

$$I_0(\theta) = \frac{I_{max}}{2\pi} \frac{2\sin\frac{\theta}{2} - \theta\cos\frac{\theta}{2}}{1 - \cos\frac{\theta}{2}} \tag{2.9}$$

$$P_{OUT,TL} = \frac{I_1 V_1}{2} = \frac{P_{RF,A}}{\pi} \frac{\theta - \sin\theta}{1 - \cos\frac{\theta}{2}} \tag{2.10}$$

$$\eta_{TL} = \frac{P_{RF,TL}}{P_{DC,TL}} = \eta_A \frac{\theta - \sin\theta}{2\sin\frac{\theta}{2} - \theta\cos\frac{\theta}{2}} \tag{2.11}$$

As an example, assuming a CCA $\theta = 180$, a PA operating in TL increases its efficiency to 57% compared to Class A operation:

$$\eta_{TL} = \eta_A \frac{\pi}{2} \tag{2.12}$$

being η_A the drain efficiency of Class A operation.

Chapter 3

CLASS F AMPLIFIER

The Class F design strategy has become a representative of the high-efficiency amplifier, offering high output power and design simplicity. It is based on the idea of tuning to open circuit the load impedance at odd harmonics and tuning to short circuit the load impedance at even harmonics [5, 13, 18]. The scheme of a Class F amplifier is depicted in figure 3.1:

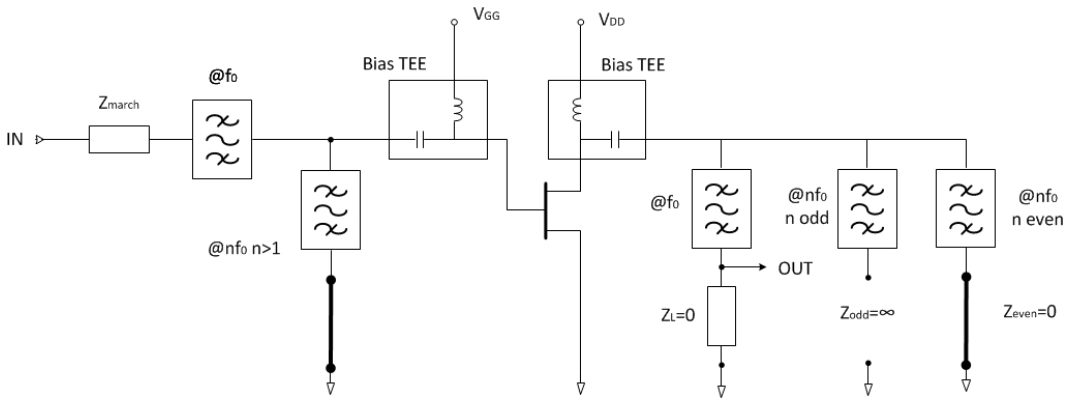

Figure 3.1: Ideal structure of a Class F amplifier.

Ideally, the drain voltage is shaped toward a square wave and drain current is shaped toward a half since wave, resulting in no internal and harmonic dissipation power, thus achieving 100 % theoretical drain efficiency [20]. The drain current $I_D(\theta)$ and voltage $V_{DS}(\theta)$ are expressed in Eqs. 3.1 and 3.2 respectively [5]:

$$I_D(\theta) = \begin{cases} I_{max}cos(\theta) & \text{if } -\frac{\pi}{2} \leq \theta \leq \frac{\pi}{2} \\ 0 & \text{otherwise} \end{cases} \tag{3.1}$$

$$V_{DS}(\theta) = \begin{cases} 0 & \text{if } -\frac{\pi}{2} \leq \theta \leq \frac{\pi}{2} \\ 2V_{DD} & \text{otherwise} \end{cases} \tag{3.2}$$

The optimum load at fundamental frequency Z_n can be calculated as:

$$Z_n = \frac{V_n}{I_n} = \begin{cases} \frac{8}{\pi}\frac{V_{DD}}{I_{max}} & n = 1 \\ 0 & n \text{ even} \\ \infty & n \text{ odd} \end{cases} \tag{3.3}$$

$$R_F = \frac{4}{\pi}\frac{2V_{DD}}{I_{max}} = \frac{4}{\pi}R_{TL} \tag{3.4}$$

The DC power $P_{DC,F}$, the output power at the fundamental frequency $P_{OUT,F}$ and the drain efficiency η_F are given by the following expressions:

$$P_{DC,F} = V_{DD}\frac{I_{max}}{2\pi}\frac{2\sin(\frac{\phi}{2}) - \phi\cos(\frac{\phi}{2})}{1 - \cos(\frac{\phi}{2})} \tag{3.5}$$

$$P_{OUT,F} = \frac{I_{max}(V_{DD} - V_k)}{\pi^2}\frac{\phi - \sin(\phi)}{1 - \cos(\frac{\phi}{2})} \tag{3.6}$$

$$\eta_F = \frac{2}{\pi}\frac{\phi - \sin(\phi)}{2\sin(\frac{\phi}{2}) - \phi\cos(\frac{\phi}{2})} \tag{3.7}$$

Output power, gain and efficiency from Class F compared to the corresponding TL figures report an improvement about 15% up to saturation when the theoretical improvement is maximum:

$$P_{OUT,F} = 1.15P_{OUT,TL} \tag{3.8}$$

$$G_F = 1.15G_{TL} \tag{3.9}$$

$$\eta_F = 1.15\eta_{TL} \tag{3.10}$$

Chapter 4

DESIGN STRATEGIES

TL and class F PA have been designed with the operating frequency at 2.4 GHz using Agilent's Advanced Design System (ADS) circuit simulator. For these amplifiers' design, the active device used is a CGH40010 GaN HEMT from Cree Corporation, a device capable of 10 W output power at 28 V drain bias and operating frequency up to 6 GHz [21]. This is appropriate for the proposed specifications. As in these amplifiers implementations a finite number of harmonics can be effectively controlled [5], in this work only the 2nd and 3rd harmonics have been considered, allowing a simplified circuit design.

The gate bias is fixed at -2.7 V in class AB condition, according to the device's I_{DS} vs. V_{GS} curve in Fig. 4.1.

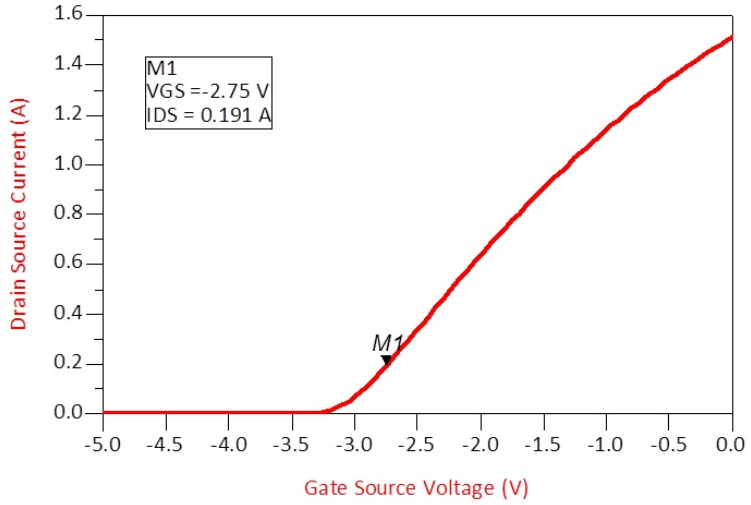

Figure 4.1: Class of operation defined by the device quiescent bias point.

For both amplifiers, two 47 pF capacitors are the DC blocking capacitors at the input and the output networks, and three 47 pF are the bypass capacitors at the gate and drain bias networks.

Bias network is used to separate the DC and RF signals paths. It has been realized using a 3-element T-network formed by $Z_0 = 50\Omega$ impedance characteristic transmission lines as shown in Fig. 4.2. As can be noticed the bias Tee represents an open-circuit for odd harmonics and a short-circuit for even harmonics.

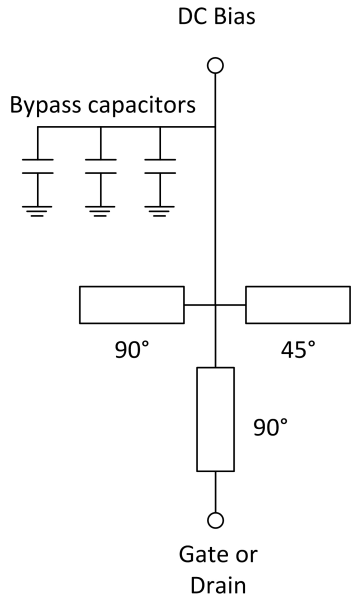

Figure 4.2: Bias Tee network.

Fig. 4.3 shows the bias Tee performance with the input reflection coefficient location for fundamental, second and third harmonics reported on the Smith chart.

The output matching network scheme of both amplifiers is presented in Fig 4.4. It consists of a compensation network where fundamental frequency is controlled, the parasitics due to the package and the second and third harmonic control.

Due to the active device internal parasitic components caused by the package, interconnections or bond wires change significantly the internal drain current and voltage waveforms from external drain current and voltage waveforms [4], the intrinsic load is obtained using the two element model parasitic extraction proposed in [22], it is based on the device equivalent circuit. In this case $L_{OUT} = 0.534$ nH and $C_{OUT} = 1.414$ pF. The device parasitic network and harmonic control network have associated the S_P scattering matrix:

$$S_P = \begin{bmatrix} S_{11,P} & S_{12,P} \\ S_{21,P} & S_{22,P} \end{bmatrix} \tag{4.1}$$

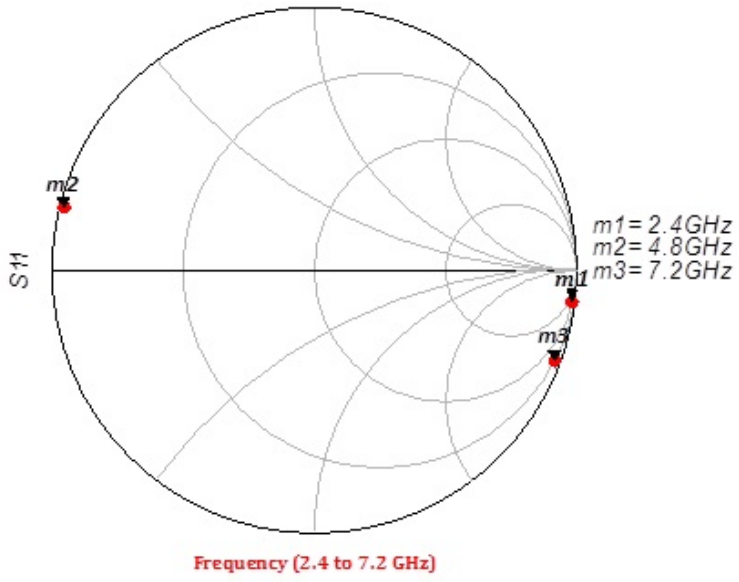

Figure 4.3: Bias Tee performance.

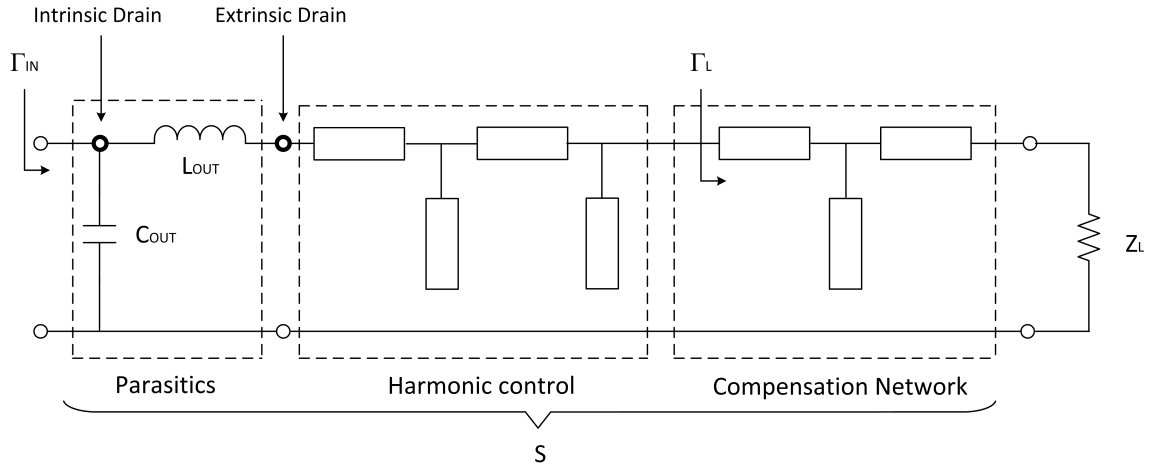

Figure 4.4: Output matching network scheme.

From Fig 4.4 if Z_L is 50Ω, Γ_{IN} must be equal to S_{11}, in Eq. 4.2, that means Γ_{IN} equals to zero [23].

$$S = \begin{bmatrix} 0 & 1 \\ 1 & 0 \end{bmatrix} \tag{4.2}$$

Thus

$$\Gamma_{IN} = S_{11,P} + \frac{S_{12,P}S_{21,P}\Gamma_L}{1 - S_{22,P}\Gamma_L} = 0 \tag{4.3}$$

and

$$S_{11,P} - S_{11,P}S_{22,P}\Gamma_L + S_{12,P}S_{21,P}\Gamma_L = 0 \tag{4.4}$$

Defining the determinant of the scattering matrix

$$\triangle_P = S_{11,P}S_{22,P} - S_{12,P}S_{21,P} \tag{4.5}$$

Solving Eq. 4.4, the value of Γ_L to be adjusted with the compensation network is expressed as:

$$\Gamma_L = \frac{S_{11,P}}{\triangle_P} \tag{4.6}$$

Due to the whole network in Fig 4.4 is lossless, immediately S_{11} equals to S_{22} and $|S_{12}| = |S_{21}| = 1$. This network has to include a third line, so that the phase of the S_{12} and S_{21} parameters is zero. The output matching networks to be synthesized have to transform the 50 Ω reference termination to the optimum value at the operating frequency, being $Z_{TL} = 30$ Ω and $Z_F = 34.5$ Ω according to Eq. 2.6 and Eq. 3.4 respectively to each amplifier.

The optimum load terminations up to third harmonic frequencies have been determined and reported in Table 4.1 and Table 4.2.

Frequency [GHz]	$Z_L[\Omega]$
0.0	38.017/-180.000
2.4	30.087/0.016
4.8	0.006/90.000
7.2	0.310/90.000

Table 4.1: Optimum load terminations up to third harmonic frequencies for TL amplifier.

Frequency [GHz]	$Z_L[\Omega]$
0.0	59.513/-180.000
2.4	34.500/0.001
4.8	0.013/-90.000
7.2	$2.262 * 10^5$/90.000

Table 4.2: Optimum load terminations up to third harmonic frequencies for class F amplifier.

The input networks are synthesized in order to guarantee maximum power transfer at the operating frequency, taking into account that the impedance source has to be the same as conjugate input reflection coefficient. Both amplifiers have been stabilized in the frequency

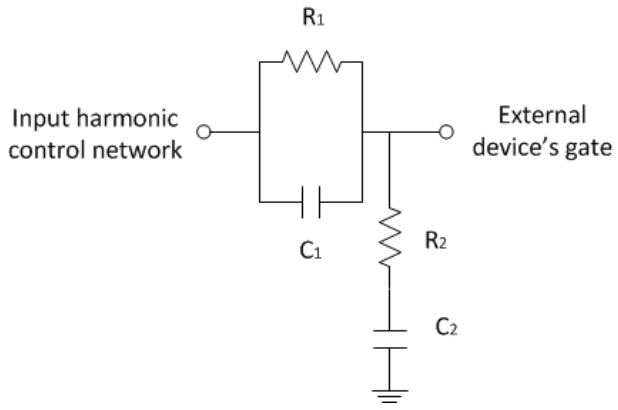

Figure 4.5: Stabilizing network.

range from 0 to 6 GHz, thanks to the same RC parallel and series networks shown in Fig. 4.5, being $R_1 = 10\ \Omega$, $C_1 = 4.7$ pF, $R_2 = 100\ \Omega$ and $C_2 = 33$ pF.

To evaluate the amplifiers stability it is used the stabFact tool in the software, which carries out a frequency sweep. As shows the Fig. 4.6, the Rollet's condition is satisfied. The complete schemes of the realized amplifiers are shown in Fig. 4.7 and Fig. 4.8. S-parameters behavior of both amplifiers are simulated and depicted in Fig. 4.9 and Fig. 4.10.

Simulated drain current and voltage waveforms in time domain are depicted in Fig. 4.11. Due to the limiting number of harmonics, the waveforms show approximate TL and class-F operation respectively. In Fig. 4.11 (b), the drain current is almost zero when the drain voltage peaks.

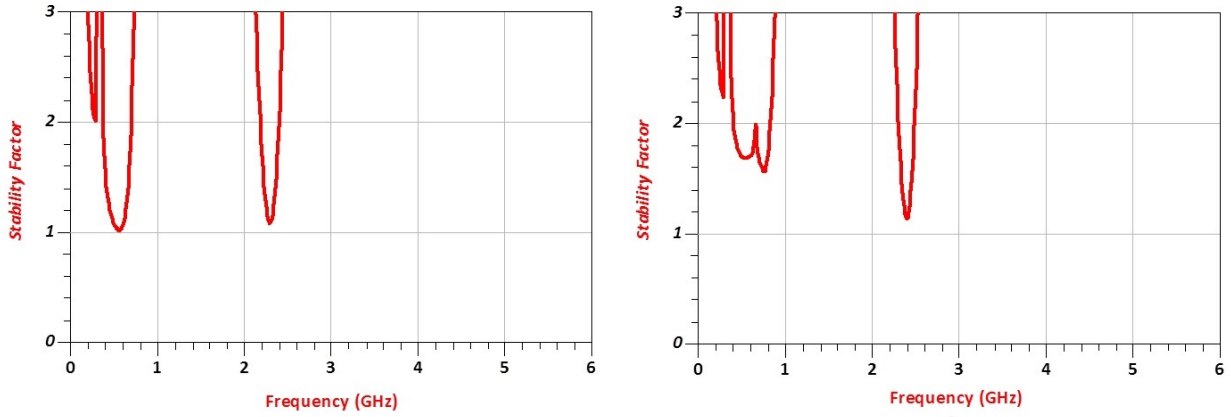

(a) (b)

Figure 4.6: Stability frequency sweep of (a) TL and (b) Class F

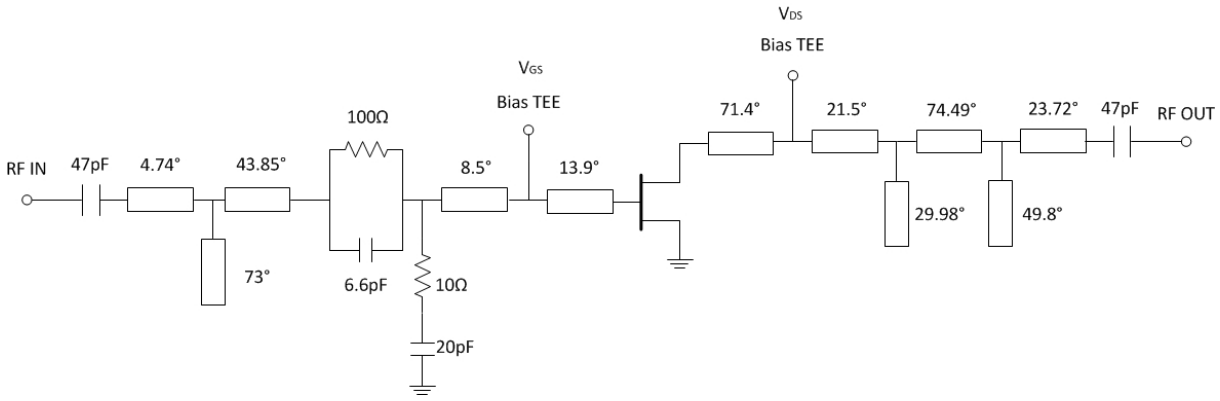

Figure 4.7: TL final scheme.

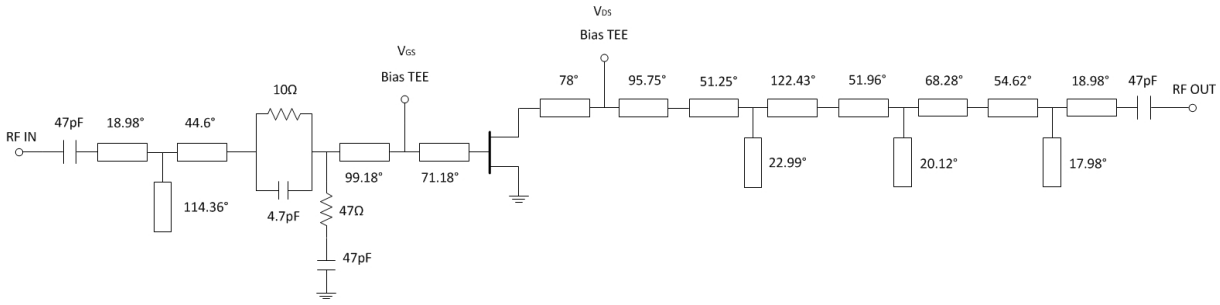

Figure 4.8: Class F final scheme.

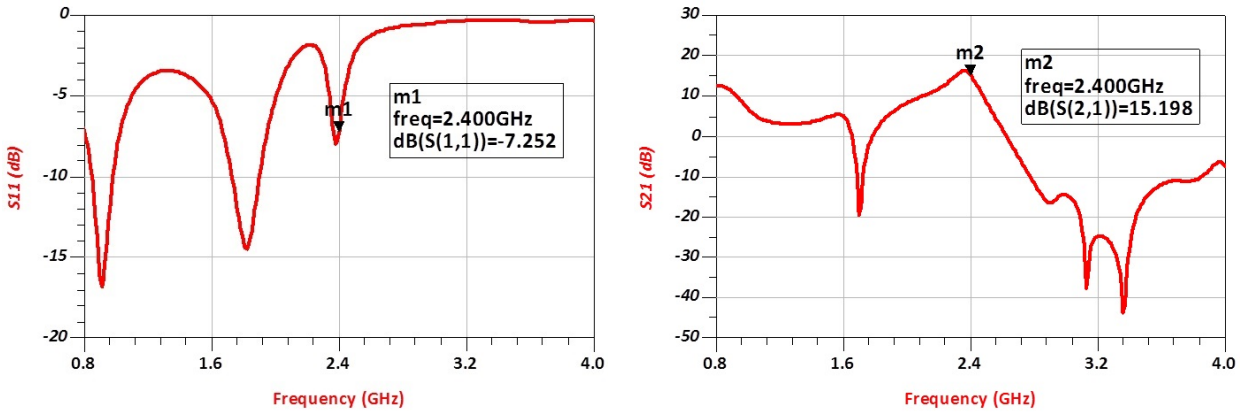

(a) (b)

Figure 4.9: Simulated S-parameters of TL: (a) S_{11} and (b) S_{21}

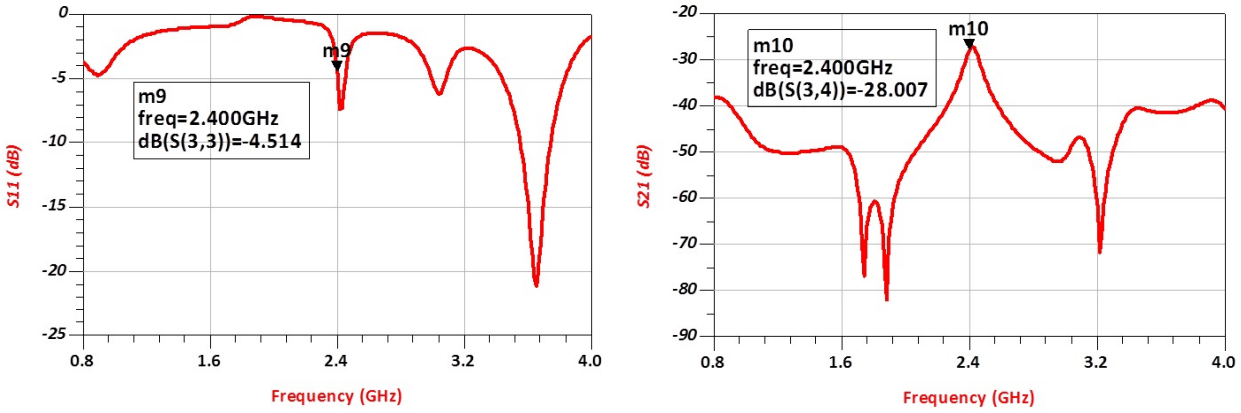

(a) (b)

Figure 4.10: Simulated S-parameters of class F: (a) S_{11} and (b) S_{21}

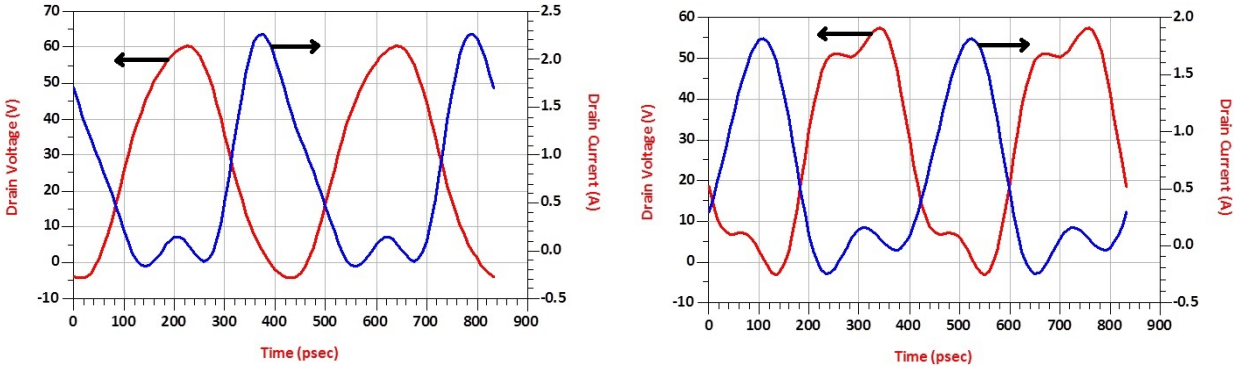

(a) (b)

Figure 4.11: Simulated drain current (blue) and voltage (red) waveforms for (a) TL and (b) class F amplifiers designed

Fig. 4.12 shows the simulated output power, efficiency and power gain for both amplifiers. TL exhibits a power gain of 15.2 dB, an efficiency of 73.3 % and an output power of 41.7 dBm. The class F operation has a power gain of 17.5 dB, an efficiency of 78.5 % and an output power of 40.8 dBm.

These results show that the TL operation delivers less efficiency and higher power than the class-F operation.

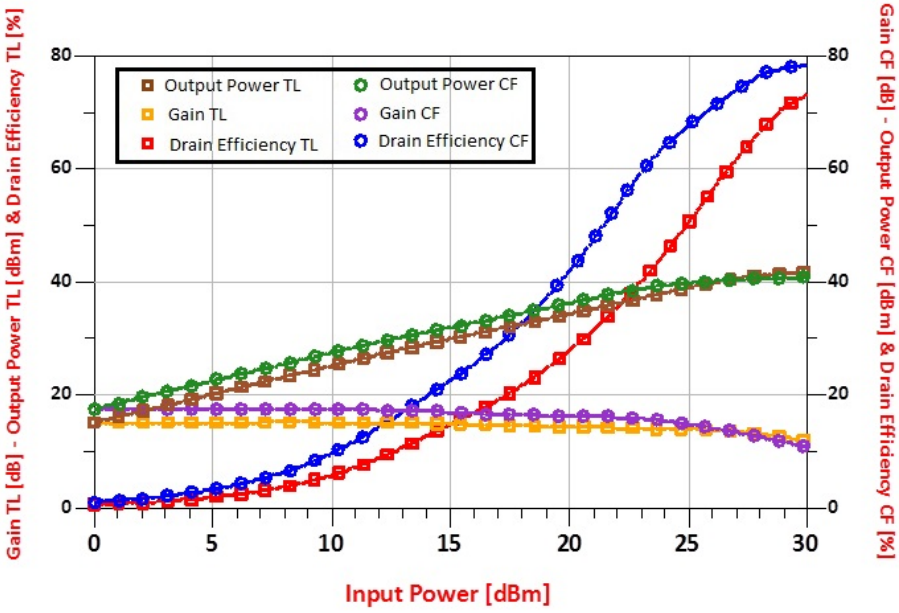

Figure 4.12: Simulated performance of TL and class F amplifiers.

Chapter 5

IMPLEMENTATION AND EXPERIMENTAL RESULTS

5.1 Implementation

Prototypes have been fabricated on a Taconic's RF35 substrate with copper metallization ($H = 760\mu m, \varepsilon r = 3.5$ and $t = 0.035mm$) and using Agilent ADS CAD. The microstrip circuit is carried out by hand. Surface-mount devices have been used.

The microstrip circuit is mounted on an adequate carrier made of conductive materials such as aluminum or brass, to ensure a properly heat dissipation [6, 24–26]. In this case three different metal sheets were tested: iron, porous aluminum and solid aluminum. The iron and porous aluminum carriers did not work, in both cases oscillations were presented. The test with the solid aluminum carrier is successful. The carrier and the active device are secured with screws to ensure good electrical and thermal contact with the microstrip and to avoid oscillations.

Considering the probes and attenuators are heavy and little flexible, some reinforcements are used to secure the input and output SMA connectors preventing the damage of the prototype. To get well-defined tracks on the circuit, especially when its very large, the input and output networks are manufactured separately in order to have greater control of the acid. A picture of the final amplifiers is presented in Fig. 5.1 and Fig. 5.2.

5.2 Small signal measurements

As the first step, the amplifiers stability is verified doing a frequency sweep that includes the fundamental frequency through the Spectrum Analyzer. To protect the equipments and

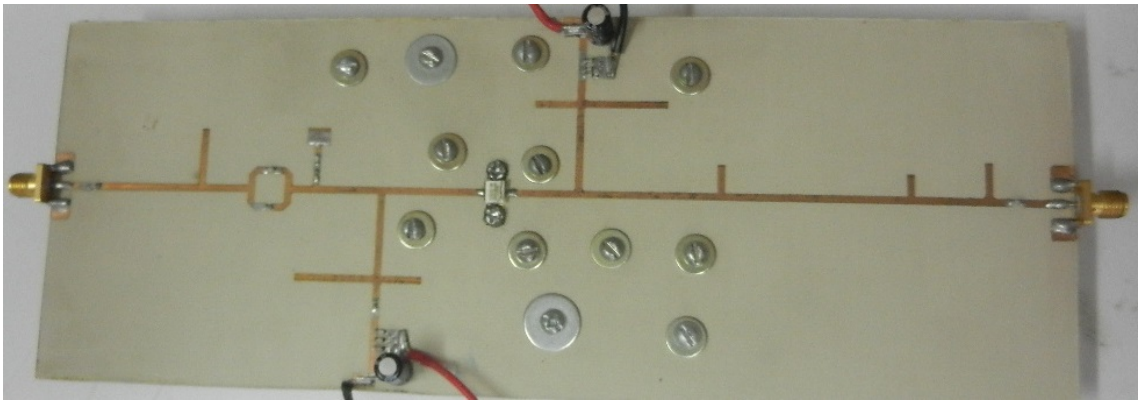

Figure 5.1: Picture of the realized TL PA.

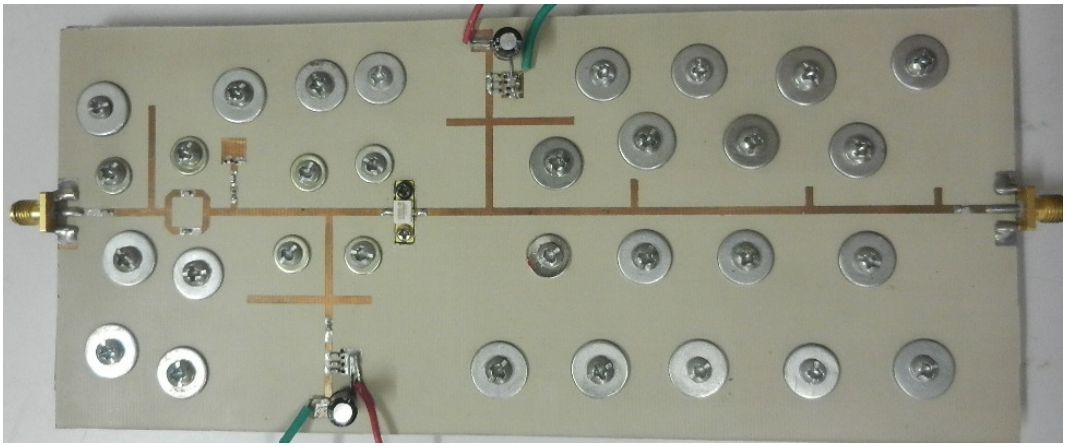

Figure 5.2: Picture of the realized Class F PA.

the devices, some attenuators are included in the measurement setup. In this case there is a total attenuation of 50 dB. The amplifiers characterization has been carried out with the experimental setup shown in Fig. 5.3 .

After the Vector Network Analyzer (VNA) is calibrated, parameters S_{11} and S_{21}, which represent input reflection coefficient and the amplifier gain respectively, are measured doing a frequency sweep from 1.5 to 4 GHz. Fig. 5.4 shows good agreement between simulated (red circle) and measured (blue triangle) S_{21} for both amplifiers, exhibiting a measured peak gain of 15.5 dB and 17.8 dB over 2.35 GHz. The frequency shift of 100 MHz is possibly due to the amplifier handmade construction.

Fig. 5.5 shows a comparison between simulated (red circle) and measured (blue triangle) parameter S_{11} for both amplifiers, resulting to have the better coupling at 2.28GHz with -8.7 dB for TL and at 2.33 GHz with -14.87 dB for Class F. It is established the operating

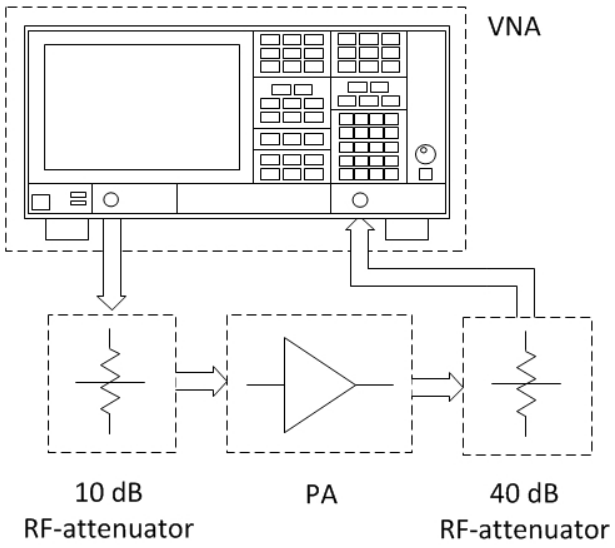

Figure 5.3: Experimental setup for the amplifiers characterization

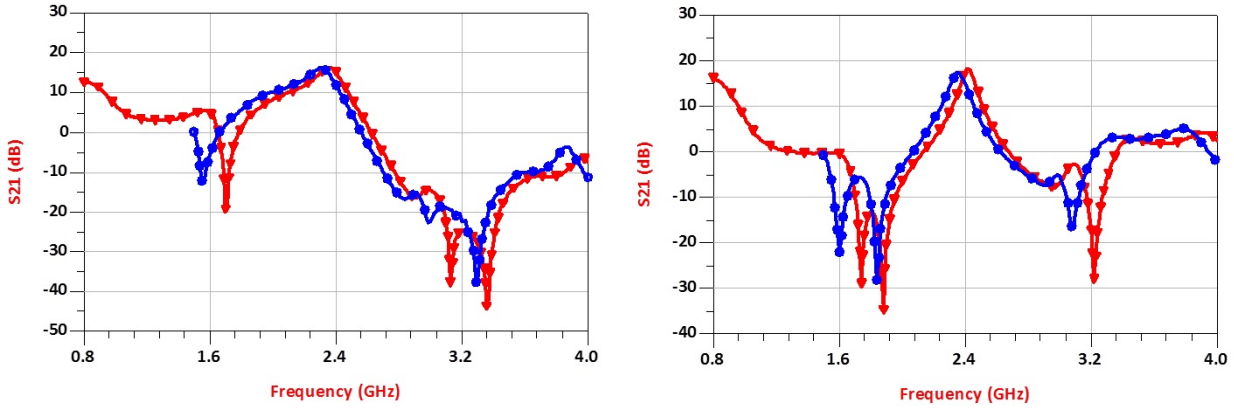

(a) (b)

Figure 5.4: Comparison of simulated (red circle) and measured (blue triangle) S_{21} for (a) TL and (b) class F

frequency at 2.35 GHz due to both amplifiers report good power gain and impedances coupling, in this case the return loss measured are -5.6 dB for TL and -11.4 dB for Class F.

5.3 Power measurements

The VNA is used as a power source to obtain output power, gain and efficiency, importing the measurement data to depict and to compare the results. The Fig. 5.6 shows the setup

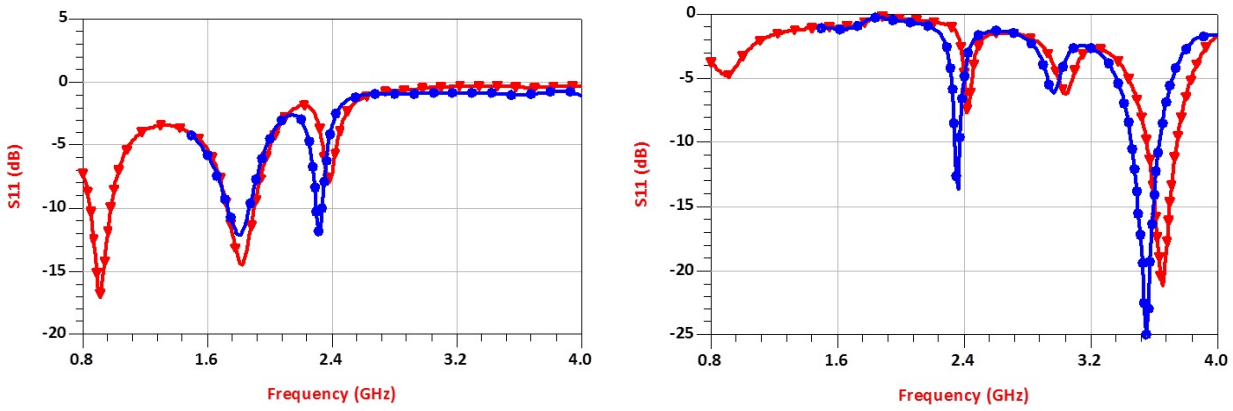

(a) (b)

Figure 5.5: Comparison of simulated (red circle) and measured (blue triangle) S_{11} for (a) TL and (b) class F amplifiers designed

for power measurement. Due to the VNA supplies up to 15 dBm, to have an appropriate measure it is necessary to use a preamplifier which provides a suitable input power sweep from 0 to 30 dBm.

Three different ways are tried to take he measurements using the NRP-Z24 power sensor from Rohde & Schwarz. Only the amplifiers characterization obtained with the latest method is show for giving the most reliable results. The ways are shortly described as follow:

1. The power sensor is used to calibrate the VNA input port in the range from 0 to 15 dBm and to acquire input and output power data through an interface in the computer to be processed in Excel obtaining gain and efficiency.
2. The power sensor is used to calibrate the VNA input port in the range from 0 to 15 dBm. The output port is calibrated as a receiver. Gain and efficiency data files delivered by VNA are processed in Excel.
3. The VNA is calibrated with the preamplifierand the attenuator for taking into account the variations of losses of these elements. Input power sweep was carried out with a 3 seg delay to stabilize the current.

Fig. 5.7 shows the performance of PAs measured. TL achieves a maximum efficiency of 52 %, corresponding to an output power of 40.9 dBm, and the gain is about 14.2 dB. In the case of Class F the output power is about 2.7 dB lower and peak efficiency is increased to 60 %, and the gain is about 16.4 dB, thus confirming the predicted theoretical improvement. Preliminary small signal measurements demonstrate a good agreement with expected results. Like S_{21} exhibits, the measured gain for both amplifiers decreases while input power increases. According to simulation, output power and gain are higher in Class F with respect to TL up to saturation.

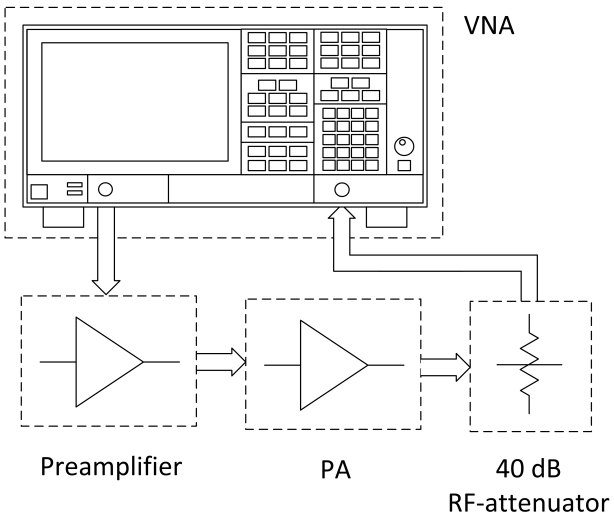

Figure 5.6: Experimental setup for the amplifiers characterization

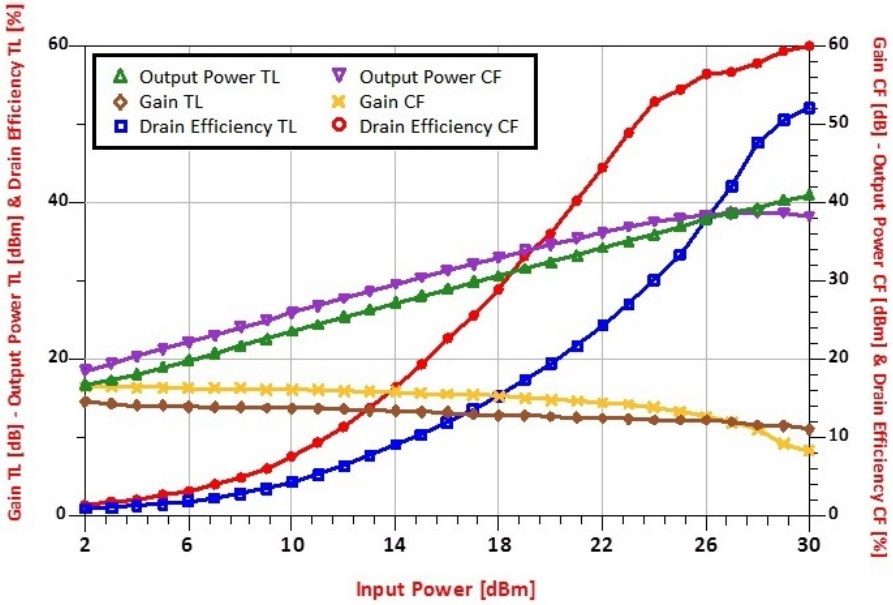

Figure 5.7: Measured performance of TL and class F amplifiers.

Table 5.1 summarizes the measured and simulated results for both amplifiers. Table 5.2 reports the proposed Class F amplifier shows superior performance compared with other works at close frequencies.

Parameter	Simulated TL	Measured TL	Simulated Class F	Measured Class F
Max Gain [dB]	15.2	14.2	17.5	16.4
Max P_{OUT} [dBm]	41.7	40.9	40.8	38.2
Max η [%]	73.3	52.0	78.5	60.0

Table 5.1: Performance comparison.

Work	Frequency [GHz]	Max G [dB]	Max P_{OUT} [dBm]	Max PAE [%]	Max η [%]
[3]	2	10	36	50.4	-
[4]	1.2	15.8	36.3	77.6	-
[6]	2.14	13	36.5	-	54
[27]	0.9	14	22	71.4	-
[28]	1	-	22.5	64	-
[29]	1	-	40.3	79.2	-
[30]	1.88	0.3	32.5	63.8	-
[31]	9.6	< 12.5	50	28.1	-
This work	2.4	16.4	38.2	50.9	60.0

Table 5.2: Class F performance comparison.

Chapter 6

CONCLUSIONS

A theoretical and experimental comparison between two high efficiency harmonics tuned microwave PAs was presented. It was carried out through the design, realization and characterization of a TL and a Class F PAs based on GaN HEMT technology operating at 2.4 GHz. The excellent simulated and measured performance were evaluated. The obtained results show higher performance for Class F with respect to TL, thus confirming the predicted theoretical improvement.

Its important to highlight this project applies a design strategy to carry out the output network and a parasitic extraction model developed by members of the group GINTEL.

This work has been used as the basis for the development of other works with regard to the design, realization and characterization of high efficiency PAs, including some at graduate level. Some of these works are:

Diseño e implementación de un amplificador Doherty a 2.4 GHz con potencia de salida mayor a 20 W.

Implementación de estrategias para el manejo eficiente de la energía en transmisores aplicados a sistemas de comunicaciones inalámbricas.

Diseño e implementación de un amplificador Doherty con etapa de preamplificación en aplicaciones WIMAX.

Diseño e implementación de dispositivos amplificadores energéticamente eficientes para aplicaciones base de sistemas de comunicaciones inalámbricas.

BIBLIOGRAPHY

[1] Bumman Kim, Junghwan Moon, and Ildu Kim. "Efficiently amplified". *IEEE Microw. Mag*, 11(5):87–100, 2010.

[2] K. Kim and R. Prasad. "4G: Roadmap and Emerging Communication Technologies". Artech House. Incorporated, 2006.

[3] S Gao, P Butterworth, A Sambell, C Sanabria, H Xu, S Heikman, U Mishra, and RA York. "Microwave class-F and inverse class-F power amplifiers designs using GaN technology and GaAs pHEMT". pages 1719–1722, 2006.

[4] Hyun-chul Park, Gunhyun Ahn, Sung-chan Jung, Cheon-seok Park, Wan-soo Nah, Byungsung Kim, and Youngoo Yang. " High-efficiency class-F amplifier design in the presence of internal parasitic components of transistors". In *Microwave Conference, 2006. 36th European*, pages 184–187. IEEE, 2006.

[5] Paolo Colantonio, Franco Giannini, and Ernesto Limiti. *High efficiency RF and microwave solid state power amplifiers*. J. Wiley, 2009.

[6] Jie Fang, J Moreno, R Quaglia, Riccardo Tinivella, V Camarchia, M Pirola, and G Ghione. "Development strategy for GaN-based high-efficiency hybrid medium-power RF amplifiers through low-cost substrate prototyping". pages 1–4, 2010.

[7] P. Colantonio, F. Giannini, E. Limiti, and V. Teppati. "An approach to harmonic load- and source-pull measurements for high-efficiency PA design". *IEEE Transactions on Microwave Theory and Techniques*, 52(1):191–198, Jan 2004.

[8] L El Maazouzi, P Colantonio, A Mediavilla, and F Giannini. "A 3.5 GHz 2nd harmonic tuned PA design". pages 1090–1093, 2009.

[9] P. Colantonio, F. Giannini, and E. Limiti. "Nonlinear approaches to the design of microwave power amplifiers". *International Journal of RF and Microwave Computer-Aided Engineering*, 2004.

[10] David M Pozar. *Microwave and RF design of wireless systems*. John Wiley & Sons, Inc., 2000.

[11] Behzad Razavi and Razavi Behzad. *RF microelectronics*, volume 1. Prentice Hall New Jersey, 1998.

[12] Guillermo Gonzalez. *Microwave transistor amplifiers: analysis and design*, volume 2. Prentice hall New Jersey, 1997.

[13] Steve C. Cripps. *RF Power Amplifiers for Wireless Communications*. Artech House, Inc., Norwood, MA, USA, 2006.

[14] A. A M Saleh and D.C. Cox. "Improving the Power-Added Efficiency of FET Amplifiers Operating with Varying-Envelope Signals". *IEEE Transactions on Microwave Theory and Techniques*, 31(1):51–56, Jan 1983.

[15] Guodong Su, Lingling Sun, Jincai Wen, Huang Wang, Zhiping Yu, and Nan Zhang. "An estimable stability method applied to power amplifier design". In *Electrical Design of Advanced Packaging and Systems Symposium (EDAPS), 2011 IEEE*, pages 1–4. IEEE, 2011.

[16] George D Vendelin, Anthony M Pavio, and Ulrich L Rohde. *Microwave circuit design using linear and nonlinear techniques*. John Wiley & Sons, 2005.

[17] Raymond S Pengelly, Simon M Wood, James W Milligan, Scott T Sheppard, and William L Pribble. "A review of GaN on SiC high electron-mobility power transistors and MMICs". *IEEE Transactions on Microwave Theory and Techniques*, 60(6):1764–1783, 2012.

[18] P Colantonio, F Giannini, and E Limiti. "HF class F design guidelines". In *Microwaves, Radar and Wireless Communications, 2004. MIKON-2004. 15th International Conference on*, volume 1, pages 27–37. IEEE, 2004.

[19] Jorge Julián Moreno Rubio, Andrés Fernando Jimenez López, and Nelson Barrera Lombana. "THE TUNED LOAD POWER AMPLIFIER". *COLOMBIAN JOURNAL OF ADVANCED TECHNOLOGIES*, 2(22), 2013.

[20] Junghwan Moon, Seunghoon Jee, Jungjoon Kim, Jangheon Kim, and Bumman Kim. "Behaviors of Class-F and Class-Amplifiers". *IEEE Transactions on Microwave Theory and Techniques*, 60(6):1937–1951, 2012.

[21] Cree Corporation. "Datasheet CGH40010". *Rev. 3.1*, 2006-2011.

[22] Julian Moreno, William Cuevas, and Edison Angarita. "Extraccion de la red parasita de la salida en dispositivos GaN-HEMT para aplicaciones en alta frecuencia". 2014.

[23] Julian Moreno, Nidia Cely, Javier Rodriguez, Juan Pachon, and Juan Espana. "Estrategia de diseno para un amplificador de potencia de alta eficiencia Clase F a 1.9 GHz". 2014.

[24] Jorge Moreno, Jie Fang, Roberto Quaglia, Vittorio Camarchia, Marco Pirola, and Giovanni Ghione. "Development of single-stage and doherty GaN-based hybrid RF power amplifiers for quasi-constant envelope and high peak to average power ratio wireless standards". *Microwave and optical technology letters*, 54(1):206–210, 2012.

[25] Jorge Moreno Rubio, Jie Fang, Roberto Quaglia, V Camarchia, M Pirola, S Donati Guerrieri, and Giovanni Ghione. "A 22W 65% efficiency GaN Doherty power amplifier at 3.5 GHz for WiMAX applications". In *Integrated Nonlinear Microwave and Millimetre-Wave Circuits (INMMIC), 2011 Workshop on*, pages 1–4. IEEE, 2011.

[26] Jie Fang, Roberto Quaglia, J Moreno Rubio, V Camarchia, M Pirola, S Donati Guerrieri, and G Ghione. "Design and baseband predistortion of a 43.5 dBm GaN Doherty amplifier for 3.5 GHz WiMAX applications". In *Microwave Integrated Circuits Conference (EuMIC), 2011 European*, pages 256–259. IEEE, 2011.

[27] Shirt Fun Ooi, Steven Gao, A Sambell, D Smith, and P Butterworth. "High efficiency class-F power amplifier design". pages 113–118, 2004.

[28] Young Yun Woo, Youngoo Yang, and Bumman Kim. "Analysis and experiments for high-efficiency class-F and inverse class-F power amplifiers". *IEEE Transactions on Microwave Theory and Techniques*, 54(5):1969–1974, 2006.

[29] Song Liu and Dominique Schreurs. "Intrinsic Class-F RF GaN Power Amplifier with a Commercial Transistor Based on a Modified "Hybrid" Approach". pages 1–3, Sept 2012.

[30] Daehyun Kang, Daekyu Yu, Kyoungjoon Min, Kichon Han, Jinsung Choi, Dongsu Kim, Boshi Jin, Myoungsu Jun, and Bumman Kim. "A highly efficient and linear class-AB/F power amplifier for multimode operation". *IEEE Transactions on Microwave Theory and Techniques*, 56(1):77–87, 2008.

[31] Elisa Cipriani, Paolo Colantonio, Franco Giannini, and Rocco Giofrè. " Theoretical and experimental comparison of Class F vs. Class F- 1 PAs". In *Microwave Integrated Circuits Conference (EuMIC), 2010 European*, pages 428–431. IEEE, 2010.